The isotopic fingerprint of the pre-industrial and the anthropogenic N2O source

T. Röckmann, J. Kaiser, C. A. M. Brenninkmeijer

**Atmospheric
Chemistry
and Physics**

The isotopic fingerprint of the pre-industrial and the anthropogenic N$_2$O source

T. Röckmann[1], J. Kaiser[1, 3], and C. A. M. Brenninkmeijer[2]

[1]Max Planck Institute for Nuclear Physics, Atmospheric Physics Division, Heidelberg, Germany
[2]Max Planck Institute for Chemistry, Air Chemistry Division, Mainz, Germany
[3]now at: Department of Geosciences, Princeton University, Princeton, USA

Abstract. We have performed high-precision measurements of the ^{18}O and position dependent ^{15}N isotopic composition of N$_2$O from Antarctic firn air samples. By comparing these data to simulations carried out with a firn air diffusion model, we have reconstructed the temporal evolution of the N$_2$O isotope signatures since pre-industrial times. The heavy isotope content of atmospheric N$_2$O is presently decreasing for all signatures at rates of about $-0.038‰\,\mathrm{yr}^{-1}$ for $^{1}\delta^{15}$N, $-0.046‰\,\mathrm{yr}^{-1}$ for $^{2}\delta^{15}$N and $-0.025‰\,\mathrm{yr}^{-1}$ for δ^{18}O. The total decrease since pre-industrial times is estimated to be about $-1.8‰$ for $^{1}\delta^{15}$N, $-2.2‰$ for $^{2}\delta^{15}$N and $-1.2‰$ for δ^{18}O. Isotope budget calculations using these trends and recent stratospheric measurements allow to isotopically characterize the present and the pre-industrial global average N$_2$O source, as well as the additional N$_2$O emissions that have caused the global N$_2$O increase since pre-industrial times. The increased fluxes from the depleted surface sources alone are insufficient to explain the inferred temporal isotope changes. In addition, the global average N$_2$O source signature is calculated to be significantly depleted today relative to the pre-industrial value, in agreement with recent indications from soil emission measurements.

1 Introduction

Nitrous oxide (N$_2$O) belongs to the group of greenhouse gases targeted by the Kyoto protocol for emission reduction. A prerequisite for effective control measures is a thorough understanding of the global atmospheric budget. In the case of N$_2$O, it is known that the predominant sources are microbial nitrification and denitrification reactions in soils and waters. Minor contributions come from biomass burning and industry, in particular nitric acid and nylon produc-

tion, and combustion in vehicles and power plants. However, the knowledge about individual source strengths is poor and lacks experimental verification. Measurements of the stable isotopic composition of atmospheric N$_2$O are increasingly considered to be an important method for better quantification of its global budget, and accordingly a wealth of experimental and modeling studies have investigated various aspects of the isotopic composition of N$_2$O in the past years (Cliff and Thiemens, 1997; Dore et al., 1998; Griffith et al., 2000; Johnson et al., 2001; Kaiser et al., 2002a, b, c; Naqvi et al., 1998; Rahn and Wahlen, 2000; Rahn et al., 1998; Röckmann et al., 2000, 2001a, b; Toyoda et al., 2001; Turatti et al., 2000; Yoshida and Toyoda, 2000; Yung and Miller, 1997). Underlying this effort is the notion that the increase of N$_2$O from pre-industrial to present levels should have left a signal in the isotopic composition. The temporal isotope trends predicted by model simulations, however, are only a few hundredths of a per mill per year (Rahn and Wahlen, 2000). Therefore, the experimental determination of a recent isotope trend from direct atmospheric measurements has not been accomplished so far, and the models themselves can only use assumptions about the temporal evolution of the N$_2$O isotope signatures.

Air trapped in Arctic and Antarctic firn and ice provides an important natural archive of the past atmospheric composition. In the case of firn air, the interstitial gas is not yet isolated in closed-off bubbles and over the long times the air remains in the firn before close-off, diffusion processes and gravitational separation change mixing and isotope ratios (Schwander et al., 1988). Thus, firn air measurements cannot be used directly to derive the atmospheric history of the trace gas signatures. Firn air diffusion models take these effects into account and allow a reconstruction of changes in the atmospheric composition from the firn profile. Our "forward" model, developed at the Laboratoire de Glaciologie et Géophysique de l'Environnement in Grenoble, France (Fabre et al., 2000; Rommelaere et al., 1997), requires atmospheric

Correspondence to: T. Röckmann
(T.Roeckmann@mpi-hd.mpg.de)

scenarios as input data and then calculates the firn profile at the time of the sampling. The most reliable input scenario can be chosen based on the agreement of the measured and modeled profiles.

In this paper, we reconstruct the isotopic evolution of atmospheric N_2O since pre-industrial times, assuming that the general shape of the time series is similar to results from a recent model study (Rahn and Wahlen, 2000). In addition to the difference between present and pre-industrial atmospheric isotope values, we could also precisely quantify the small present isotope trends that have not been measurable directly in the atmosphere. Global budget calculations are then used to derive the global average isotope signatures of the present and pre-industrial N_2O emissions and, by mass balance, also the source signatures of the additional emissions since pre-industrial times. In the following, we term this contribution "anthropogenic" although also changes in natural emissions, e.g. due to climatic changes, may have contributed. In this respect, we establish five important cornerstones for future isotope research on atmospheric N_2O, namely the difference between present and pre-industrial atmospheric N_2O isotope values, the present atmospheric trends, and the present, pre-industrial and anthropogenic average source signatures.

2 Experimental procedures

Within the framework of the European Project FIRETRACC (Firn Record of Trace Gases Relevant to Atmospheric Chemical Change), 16 large volume air samples were obtained in Dronning Maud Land (DML) in January 1998, and 13 samples were obtained at Dome Concordia (Dome C) in January 1999. In the laboratory, N_2O mixing ratios were determined gas chromatographically using an electron capture detector (GC-ECD). Two laboratory reference gases were used with N_2O mixing ratios of nominally 315.71 nmol/mol and 309.85 nmol/mol, respectively, on the NOAA/CMDL scale. The non-linearity of the detector was accounted for by fitting the response function to a dilution series. The DML samples were analyzed three times, two times in 1998 after arrival in the laboratory, shortly after the GC-ECD had been set up, and again in 1999 together with the Dome C samples after improvement of the system. Whereas the internal (i.e. instrumental) precision is similar for the individual analyses, the reduced scatter of the 1999 data (Fig. 1) indicates that these data are more reliable, although the air had been stored in the cylinders for more than one year. This may be due to improvements in sample handling and admission procedures. The minor differences do not affect any of the conclusions drawn below.

The ^{18}O and position dependent ^{15}N analyses were carried out using recently developed continuous-flow isotope mass spectrometric techniques (Brenninkmeijer and Röckmann, 1999; Röckmann et al., 2001a). The Dome C samples were

analyzed in the same manner that was used previously for stratospheric samples (Röckmann et al., 2001a) and only a brief summary is given here. 170 to 420 cm^3 of firn air were introduced into a modified ThermoFinnigan PreCon system, where the majority of the CO_2 is chemically removed over Ascarite (NaOH coated silica) and the N_2O is preconcentrated cryogenically. Final separation from the remaining traces of CO_2 occurs on a capillary GC column (PoraPlot, 0.32 mm i.d., 25 m) after focusing the sample on the column head. In our new setup the column is divided into a precolumn and an analytical column, which considerably reduces interferences from other atmospheric compounds, in particular on mass 31 for the NO^+ fragment (Röckmann et al., 2003). Two consecutive runs are performed, the conventional N_2O measurement collecting the ion masses 44, 45 and 46, and the NO^+ fragment measurement at masses 30 and 31 (Brenninkmeijer and Röckmann, 1999; Röckmann et al., 2001a). As sample size was no restriction for the large firn air samples, many measurements were performed on each sample (up to 10), resulting in very precise and robust results. As laboratory reference gas we use an atmospheric air sample with an N_2O mixing ratio of 315.1 nmol/mol and isotope ratios of $\delta^{15}N$ = 6.7‰ vs. atmospheric N_2 and $\delta^{18}O$ = 44.6‰ vs. VSMOW (Vienna Standard Mean Ocean Water). The mass spectrometer running gas (N_2O, purity 99.9999%) has an isotopic composition of $\delta^{15}N$ = 0.4‰ vs. atmospheric N_2 and $\delta^{18}O$ = 39.1‰ vs. VSMOW.

For the DML samples, the original air samples were exhausted, but the condensable components (primarily CO_2, N_2O and hydrocarbons) had been recovered during previous large volume (~ 400 dm^3) extractions on an offline laboratory extraction line used for CO isotope measurements (Brenninkmeijer et al., 2001). Aliquots of these condensable trace gas cocktails were introduced into the extraction system on a modified ThermoFinnigan Gasbench setup. The concentrate was purged by a helium carrier gas into a sample loop using a double-hole needle, and the contents of the loop was then injected into the extraction unit, which again consisted of a chemical CO_2 trap and cryogenic preconcentration of the N_2O, followed by GC separation as described above. Sample sizes injected were similar to those from the whole air extractions. Details of this method will be published elsewhere (Röckmann et al., 2003).

3 Results and discussion of firn air analyses

The firn air profiles from Dronning Maud Land (DML) and Dome Concordia (Dome C), for all signatures are shown in Fig. 1. DML has a mean annual temperature of $-38°C$ and a relatively high snow accumulation rate of 60 kg m^{-2} yr^{-1} (6 cm water equivalent yr^{-1}) whereas Dome C is an extremely cold site ($-53°C$) with a low snow accumulation rate (30 kg m^{-2} yr^{-1}). The firn-ice transition zone in DML is lo-
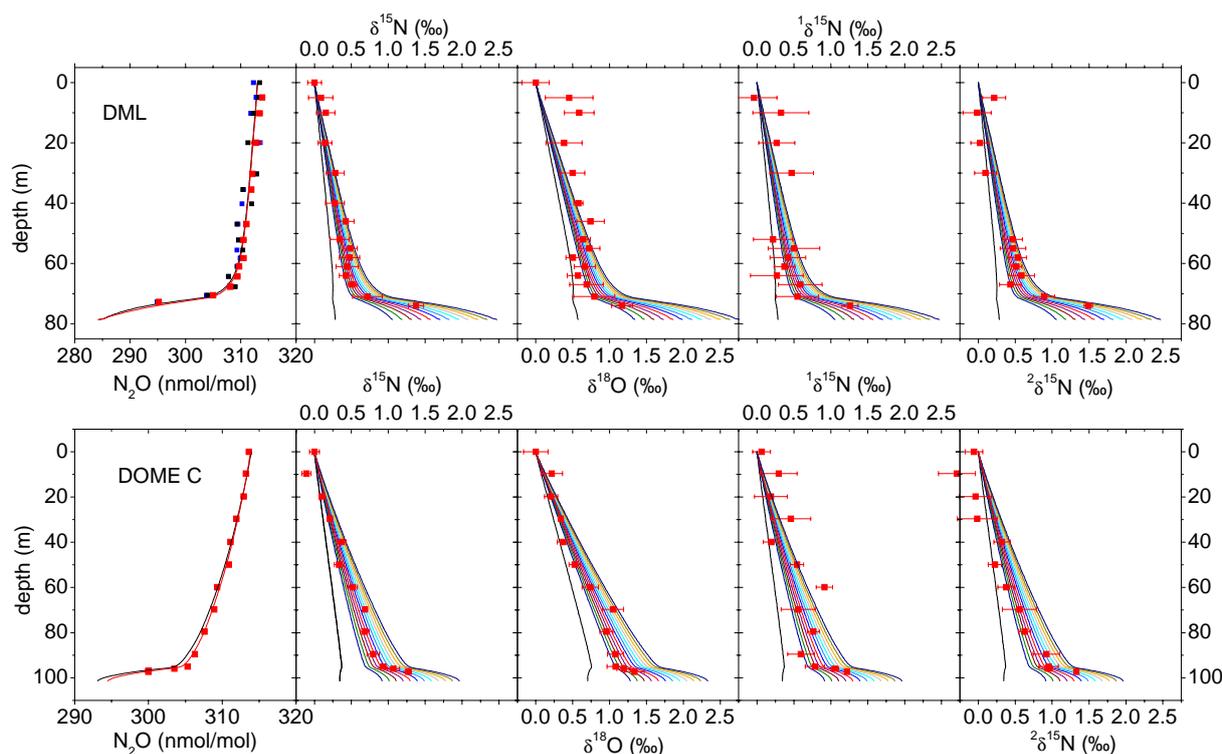
Fig. 1. Depth profiles of N₂O mixing ratio and isotopic composition at two Antarctic sites, Dronning Maud Land (top) and Dome C, together with the results from the firn air diffusion model. In the top left panel, the results of all three measurement series are presented, the black and blue squares designate the 1998 measurements, and the red squares the 1999 measurements that were carried out together with the Dome C samples. For N₂O mixing ratios, the black line is the model result using the scenario based on ice, South pole firn and atmospheric measurements, the red line is the result using the exponential model scenario (see text). The isotope ratios are reported relative to the contemporary isotopic composition at the sampling sites. $^1\delta^{15}$N and $^2\delta^{15}$N are the ^{15}N δ-values at the terminal and central position in the molecule, respectively (Brenninkmeijer and Röckmann, 1999). The trends are in good agreement to those reported recently from South Pole firn air (Sowers et al., 2001). The lines are results from the firn model using the scenarios shown in Fig. 2 as input (the colors for the scenarios match those from Fig. 2). For the isotope ratios, the black lines are profiles for a scenario without any change in isotopic composition since pre-industrial times.

cated at about 73.5 m, compared to about 99.5 m at Dome C. Although the firn-ice transition is located at shallower depth at DML, the mean age for the sample from greatest depth is actually larger than at Dome C. Furthermore, the age distributions for a certain depth level (not shown) at Dome C are broader than those at DML.

It is evident that N₂O mixing ratios decrease with depth, in accordance with the atmospheric evolution, whereas the isotope ratios increase with depth, already indicating that N₂O has become isotopically more depleted since pre-industrial times. However, as mentioned above, the raw data from the firn air measurements do not represent the actual history of the atmospheric composition due to the complicating effects of gravitational separation and diffusion. A forward firn air diffusion model has been used to calculate firn air profiles of N₂O mixing and isotope ratios based on model scenarios for the atmospheric evolution. The diffusivity profile used is the one calculated for CO₂ for this site, which is reasonable because both gases exhibit a similar quasi-exponential

increase in mixing ratio and have similar molecular properties. The slightly different diffusion coefficient for N₂O relative to CO₂ (D(N₂O) $= 1.004 D$(CO₂) Trudinger et al., 1997) has been taken into account.

Two scenarios have been used for the N₂O mixing ratio from 1700 to 2000 (Fig. 2). The first one is derived from an interpolation of ice core data (Flückiger et al., 1999), firn air measurements (Battle et al., 1996) and direct observations from the ALE/GAGE/AGAGE measurements at Cape Grim, Tasmania, available at http://cdiac.esd.ornl.gov/ftp/ale_gage_ Agage/AGAGE/gc-md/complete/tasmania. The second scenario is a simple exponential model, fit through the observed present rate of change and the pre-industrial and present mixing ratios (Kaiser, 2002). For the DML site, the firn air profile calculated from both scenarios matches the observations very well (Fig. 1). For Dome C the modeled N₂O concentrations decrease slightly faster with depth than the observed ones, which means that N₂O diffuses down to lower depth slower in the model than in reality. Such a discrepancy may
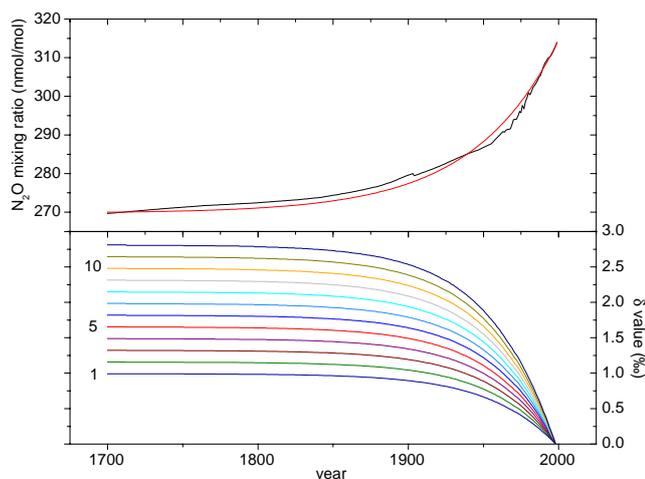
Fig. 2. Scenarios for the past evolution of atmospheric N$_2$O mixing and isotope ratios as used in the model. The black N$_2$O time series is an interpolation of a Monte-Carlo simulation based reconstruction from ice core and firn data as well as direct observations (see text). The red line is an exponential model matching the observed present rate of change and the pre-industrial and present mixing ratios. The isotope scenarios are based on the "depleted ocean" scenario (red line, number 5) from Rahn and Wahlen (2000). The whole range of scenarios is created by scaling the time series for the "depleted ocean" scenario up and down in steps of 10% of the total difference between the present and pre-industrial values. For reference, the isotope scenarios are numbered from bottom to top as number 1 through 12.

arise from adopting the same diffusivity profile for N$_2$O and CO$_2$ if, for example, interactions between the trace gas and the firn play a role. We note that CO$_2$ is more soluble in water than N$_2$O, but such an effect should be more important at the warmer DML site. Hence, the origin of the small deviation is not yet understood, but the obtained agreement between model and observations is satisfactory. The exponential model actually matches the data better than the one based on the ice core measurements, which could also mean that the South pole firn air profile (Battle et al., 1996) used for the construction of the atmospheric scenarios in the relevant time span disagrees with the Dome C profile.

For the isotope ratios, atmospheric scenarios were constructed based on recent model results by Rahn and Wahlen (2000). Whilst the general shape of their isotope scenario was maintained, it was scaled to match the firn air data as closely as possible (Fig. 2). This is equivalent to adjusting the difference between the pre-industrial and the present isotopic composition of atmospheric N$_2$O and yields the pre-industrial atmospheric N$_2$O isotope signature as a straightforward result.

As is evident from the profile of the N$_2$O mixing ratios, the most stringent constraints on the temporal evolution of the isotope signatures in the past come from the deepest samples.

Even down to 70 m for Dome C and 67 m for DML, the mean age of the air is still less than 10 years (age spectra not shown). The top part is additionally affected by thermal diffusion, which can introduce larger variations on a seasonal time scale which are not accounted for in the model.

The scenarios without any change in the isotopic composition (black lines in Fig. 1) show the effects of fractionation due to gravitational separation and diffusion alone on the N$_2$O isotopic composition in the firn. Clearly, these model runs are not in agreement with the observations. The scenarios presented in Fig. 2b result in firn profiles that are much closer to the measurements, and the oldest samples are used to select the scenarios that fit the data best. Note that the firn air data provide constraints only for the last ~ 50 years of the scenarios presented in Fig. 2 (the mean age of the oldest sample from DML is roughly 35 years). This is the period where about 2/3 of the total isotope shift occurred. Prior to this the scenarios are constrained by maintaining the general shape of the isotope evolution from (Rahn and Wahlen, 2000). The best match between the firn air model and the observed profiles is obtained for an overall decrease from 1700 to 2000 of about -2.0‰ for δ^{15}N and about -1.2‰ for δ^{18}O. The ^{15}N depletion is distributed quite evenly between the two positions; the decrease is about -1.8‰ for $^1\delta^{15}$N and -2.2‰ for $^2\delta^{15}$N. Consistent results are found for both locations. Uncertainty ranges can be estimated from the range of scenarios that agree with the data within the experimental error bars and are shown in Table 1. These isotope changes represent the isotopic fingerprint of the global average source responsible for the increase of the N$_2$O mixing ratio since pre-industrial times. From the scenarios used as input for the firn model we infer that in 1998 the isotope signatures have been changing at a rate of approximately -0.038‰ yr^{-1} for $^1\delta^{15}$N, -0.046‰ yr^{-1} for $^2\delta^{15}$N, -0.041‰ yr^{-1} for the average δ^{15}N and -0.025‰ yr^{-1} for δ^{18}O (see Table 1 for ranges). These trends are well-constrained by our measurements. Despite their small magnitude, the present isotope trends derived from the firn data are important parameters for the construction of global N$_2$O isotope budgets, because they affect the entire atmospheric N$_2$O reservoir (see below).

4 Global isotope budget calculations

Mass balance requires that the N$_2$O production from all sources $\overline{P} = \Sigma P_i = 16.4$ Tg N yr^{-1} is equal to the stratospheric loss $L_S = 12.6$ Tg N yr^{-1} plus the observed trend in the troposphere ΔT. ΔT is the tropospheric fraction ($\sim 85\%$, Warneck, 1999) of the total atmospheric annual increase of 3.8 Tg N yr^{-1} (annual fluxes are for 1998 from the Third IPCC Assessment Report; Houghton et al., 2001). The stratospheric loss term is the difference between the troposphere-stratosphere flux F_{T-S} and the stratosphere-troposphere flux F_{S-T}, leading to:

$$\overline{P} = \Sigma P_i = \Delta T + L_S = \Delta T + F_{T-S} - F_{S-T} \tag{1}$$

Table 1. Best estimates and possible ranges for the differences between present and pre-industrial atmospheric N$_2$O isotope values and for present annual isotope trends, derived from the scenarios used in the firn air model. The ranges reported here represent the range of model scenarios from Fig. 2 for which the firn profile results bracket the experimental error bars of the bottom samples (Fig. 1); model errors are not included. The scenario numbers in the last column correspond to Fig. 2

| | $\delta_{\text{present}} - \delta_{\text{preind}}$ (‰) | | present annual trend (‰ yr^{-1}) | | scenario |
	best estimate	range	best estimate	range	numbers
$^1\delta^{15}$N	−1.8	−1.5 to −2.2	−0.038	−0.032 to −0.046	4–8
$^2\delta^{15}$N	−2.2	−2.0 to −2.5	−0.046	−0.042 to −0.053	7–10
δ^{18}O	−1.2	−1.0 to −1.5	−0.025	−0.021 to −0.031	1–4
δ^{15}N	−2.0	−1.8 to −2.2	−0.041	−0.038 to −0.046	6–9

For the individual isotopologues, the fluxes are multiplied by the δ values to obtain flux-weighted isotope budgets. F_{T-S} has a typical tropospheric isotope value δ_T and the F_{S-T} has a representative stratospheric isotopic composition δ_S. The tropospheric isotope signatures are changing with time as evident from the firn air measurements, and this change has to be considered. The rate of change in the tropospheric isotope content is $\frac{d(T \cdot \delta_T)}{dt} = \delta_T \frac{dT}{dt} + T \frac{d(\delta_T)}{dt}$. Here, T is the tropospheric share (85%, Warneck, 1999) of the atmospheric N$_2$O inventory of 1510 Tg N in 1998 (Houghton et al., 2001), i.e. $T = 1284$ Tg N, and δ_T is the isotopic composition of tropospheric N$_2$O. Thus, the globally averaged source signature $\bar{\delta}$, which is the flux-weighted average of all individual source signatures δ_i, can be calculated from:

$$\overline{P\delta} = \Sigma P_i \delta_i = \delta_T \frac{dT}{dt} + T \frac{d(\delta_T)}{dt} + (F_{T-S}\delta_T - F_{S-T}\delta_S) \quad (2)$$

The calculations can be further simplified and are more illustrative if δ is expressed relative to the tropospheric average rather than to an international reference material. The rescaled values $\delta'_x (x = i, T, S)$ are derived from the δ_x values versus a reference material as $\delta'_x = (\delta_x - \delta_T)/(1 + \delta_T)$. Thus, $\delta'_T = 0$ by definition, and Eq. (2) reads

$$\overline{P\delta'} = \frac{T}{1 + \delta_T} \frac{d(\delta_T)}{dt} - F_{S-T}\delta'_S \quad (3)$$

The most critical point in the budget calculations is the estimation of F_{S-T}. Assuming that the average exchange flux of total air between stratosphere and troposphere F is equal in both directions, $F_{T-S} = F \cdot \mu_T$ and $F_{S-T} = F \cdot \mu_S$, where μ_T and μ_S are the tropospheric N$_2$O mixing ratio and a stratospheric mixing ratio representative for the air returning from the stratosphere, respectively. Thus, $L_S = F(\mu_T - \mu_S)$. In a simple two-box model of the atmosphere, the second necessary relation between F and μ_S can be derived from basic atmospheric quantities as $\mu_S = \mu_T \cdot (F\tau - N\chi_T)/(F\tau + N\chi_S)$ (Kaiser, 2002). Here, $N = 1.77 \cdot 10^{20}$ mol is the total number of molecules in the atmosphere (Trenberth and Guillemot, 1994), τ is the global atmospheric lifetime of N$_2$O of about 120 yr, $\mu_T =$

314 nmol/mol is the tropospheric N2O mixing ratio in 1998 and $\chi_S = 0.15$ and $\chi_T = 0.85$ are the fraction of air in the stratosphere and troposphere, respectively (Warneck, 1999). Using $L_S = 0.45$ Tmol yr^{-1} for the stratospheric annual loss (Houghton et al., 2001), these simple calculations yield $F = 0.22$ Tmol s^{-1} for the total flux between stratosphere and troposphere and $\mu_S = 248$ nmol/mol for the N$_2$O mixing ratio of the air returning from the stratosphere. Holton (1990) calculated the flux across the 100 mb isobar (corresponding to $\chi_S \approx 0.1$) and found $F = 0.20$ Tmol s^{-1}, which corresponds to $\mu_S = 243$ nmol/mol for his value of $\mu_T = 330$ nmol/mol. Our value of $\mu_S = 248$ nmol/mol value is also consistent with $\mu_S = 250$ nmol/mol that was used in recent studies of air mass exchange between stratosphere and troposphere (Luz et al., 1999). Adopting $F = 0.22$ Tmol s^{-1} and $\mu_S = 250$ nmol/mol from the above calculations yields values of $F_{T-S} = 61.1$ Tg N yr^{-1} (in good agreement with 60 Tg N yr^{-1} from Holton, 1990) and $F_{S-T} = 48.5$ Tg N yr^{-1}.

The values of δ'_S, i.e. the stratospheric isotope ratios corresponding to a mixing ratio of 250 nmol/mol, can be calculated from recent stratospheric N$_2$O isotope measurements (Röckmann et al., 2001a), and are given in Table 2. We note that although there is still considerable discussion about the true value of F, the isotope budget calculations below are not very sensitive to the choice of its precise value. If a smaller value for F is chosen, then the N$_2$O in the stratosphere is exposed to the stratospheric sink for a longer time and will get more enriched, i.e. less N$_2$O is returned from the stratosphere, but with a higher isotope enrichment. Conversely, if F is larger, the stratospheric N$_2$O has less time to be fractionated in the stratosphere and will therefore be less enriched. The isotope flux ($F_{S-T} \cdot \delta'_S$) is thus not as sensitive to F as the flux F_{S-T} itself.

Now all isotope fluxes on the right hand side of Eq. (3), i.e. the sink terms and the tropospheric trends, are known and the source terms for the present atmosphere can be calculated. The results in Table 2 show that the global average source is strongly depleted versus the tropospheric average, as expected since the source emissions have to counteract the

Table 2. Fractionation constants ε_{app} for the lower stratosphere and representative stratospheric isotope enrichments for a mixing ratio of 250 nmol/mol ($\delta'_{strat,250nmol/mol}$) are based on the stratospheric measurements from (Röckmann et al., 2001a). Using these stratospheric enrichments and the trends from the firn data, we calculate δ values of the modern global average N$_2$O source, $\overline{\delta'}_{modern}$. The ranges are based on the ranges derived for the atmospheric trends (Table 1). Results without incorporation of these trends are also shown. Similar calculations for the pre-industrial atmosphere yield the global average source signature in pre-industrial times versus $\delta_{T,preind}$. Using the difference between the present and pre-industrial value of δ_T from the firn air measurements (Table 1), we calculate the pre-industrial source signature versus the modern atmospheric signature (column 8), which allows a direct comparison between the present and the pre-industrial global average N$_2$O source. To calculate the isotopic fingerprint of the anthropogenic contribution, two values are adopted for its source strength: The difference between the present source and the calculated pre-industrial one, 5.6 Tg N yr^{-1} (see text), which is in good agreement with the IPCC-2 assessment (5.7 Tg N yr^{-1}), and the revised value from the IPCC-3 assessment (Houghton et al., 2001) of 6.9 Tg N yr^{-1}, which requires a reduction of the natural source to 9.5 Tg N yr^{-1} for a closed budget. The isotope results for the two different values of the anthropogenic source strength differ only slightly

	ε_{app} (‰)	$\delta'_{strat,250nmol/mol}$ (‰)		$\overline{\delta'}_{modern}$ (‰)		$\overline{\delta'}_{preind}$ (‰)		$\overline{\delta'}_{anthr}$ (‰)	
		vs. δ_T	vs. $\delta_{T,modern}$	range	no present trends	vs. $\delta_{T,preind}$	vs. $\delta_{T,modern}$	IPCC-2	IPCC-3
terminal ^{15}N	12.9	2.95	−12.1	−11.6 to −12.8	−9.0	−11.3	−9.5	−17.8	−15.5
central ^{15}N	21.3	4.83	−18.5	−18.2 to −19.1	−14.8	−18.6	−16.5	−22.8	−21.1
^{18}O	14.0	3.20	−11.8	−11.5 to −12.3	−9.8	−12.3	−11.1	−13.3	−12.7
^{15}N	17.1	3.89	−15.3	−15.0 to −15.7	−11.9	−15.0	−13.0	−20.1	−18.2

stratospheric enrichments. The consideration of the small annual trends derived from the firn air measurements above is important. Table 2 also shows results of budget calculations ignoring these trends, as done in some previous global N$_2$O isotope budget calculations (Kim and Craig, 1993; Yoshida and Toyoda, 2000). Clearly, the resulting source signatures are much heavier then.

Similar isotope budget calculations can also be performed for the pre-industrial atmosphere. Here, Eq. (3) simplifies further if we assume that the global N$_2$O budget as well as the N$_2$O isotopic composition were then in equilibrium, i.e. $P = L$ and $\frac{d(\delta_T)}{dt} = 0$. We furthermore make the assumptions that the N$_2$O lifetime, the stratospheric fractionation constants ε and the total exchange of air between troposphere and stratosphere F have remained invariable since 1700, so that the sink strength can be scaled down from its present value of 12.6 Tg N yr^{-1} at 315 nmol/mol N$_2$O to a pre-industrial value of 10.8 Tg N yr^{-1} at 270 nmol/mol. Likewise, F_{T-S} can be scaled down to 52.4 Tg yr^{-1} and thus $F_{S-T} = 41.6$ Tg yr^{-1}. In these calculations, the resulting values of δ' are relative to the pre-industrial, not the present tropospheric N$_2$O isotopic composition. For direct comparison to the present day results, the differences between the present and the pre-industrial atmosphere as derived above from the firn air measurements have to be taken into account (Table 2).

A comparison of the pre-industrial and the present source signatures in Table 2 shows that the isotopic composition of the global average N$_2$O source has significantly decreased between the pre-industrial and present atmospheres. The decrease is smallest for δ^{18}O, which has the smallest

stratospheric fractionation constants and the smallest present trend, and largest for $^2\delta^{15}$N, for which the stratospheric fractionation and the trend are strongest. It is not clear a priori that the signatures have to get isotopically depleted, since the atmosphere at present is no longer in a source – sink equilibrium. Even without a change in the global average isotope signature, the strong increase in the flux of the depleted source emissions would lead to a decrease in the atmospheric δ values, because the stratospheric return flux F_{S-T} has not increased proportionally, i.e. the source and sink terms in Eq. (3) do not match. The budget calculations clearly show, however, that an additional decrease in the global average source signature is required to explain the differences between the present and pre-industrial N$_2$O isotope values in the atmosphere. These important constraints on the temporal evolution of the global average source signature come in particular from the incorporation of the present isotope trends that are derived from the firn air measurements. If the trends are not included, the present global average isotope signature would actually be heavier than the pre-industrial one (Table 2). This is also easy to understand from Eq. (3): If $\frac{d(\delta_T)}{dt} = 0$ is prescribed, the absolute magnitude of $\overline{\delta'}$ has to be reduced when the total source flux $\overline{P}$ increases and F_{S-T} does not increase proportionally.

We note that in particular the trend to isotopically depleted values between pre-industrial and present source signatures is not very sensitive to small changes in individual parameters of the calculations (e.g. the stratospheric enrichments or the stratosphere-troposphere fluxes). In addition to the above discussion on the evaluation of F_{S-T} (following Eq. 3), in this comparison both the present and the pre-industrial

inventories are affected. However, the budget calculations show that if strongly different values for the stratospheric enrichments are used (Griffith et al., 2000), the global average source signature ends up close to the lowest ever measured source data, providing additional evidence that those stratospheric fractionation factors are too large.

Having derived the isotope signatures of the present and pre-industrial N$_2$O sources, a simple mass balance equation can be used to calculate the isotope signature of the anthropogenic source, assuming that the natural contribution has not changed. The results in Table 2 show that the total anthropogenic source, which accounts for the difference between the pre-industrial and present emissions, is considerably depleted relative to the pre-industrial source. The results differ only slightly for two different values of the anthropogenic source strength.

Thus, global N$_2$O isotope budget calculations using measured stratospheric fractionation constants and the temporal atmospheric isotope trends allow to identify the isotopic fingerprint of the present, the pre-industrial and the anthropogenic global average N$_2$O sources. Together with the derived temporal trends in the troposphere, these are important foundations for budgetary isotope research on N$_2$O, and we present some first conclusions: The fact that anthropogenic emissions are significantly depleted relative to the pre-industrial N$_2$O source is likely a result of several factors. First, the pre-industrial sources include the isotopically enriched oceanic emissions. On the other hand, also anthropogenic sources include rather enriched industrial emissions from fossil fuel combustion, nylon production and nitric acid production. The isotope signatures of these industrial emissions are only poorly known, but apparently their combined effect on the anthropogenic source is less than that of oceanic emissions on the pre-industrial source. Furthermore, recent soil measurements indicate that N$_2$O from agricultural soils is even more depleted than natural soil emissions (Pérez et al., 2001). This is supported by the present budget calculations: If we subtract the contribution of the oceanic source from both the pre-industrial and the present average source signatures, the isotope values for the remaining sources are similar. For the pre-industrial source, these remaining sources are mainly soil emissions, whereas for the anthropogenic source the relatively enriched industrial emissions contribute. Therefore, soil derived N$_2$O emissions must be even more depleted today than in the pre-industrial era.

5   Conclusions

Isotope measurements on N$_2$O from Antarctic firn air samples show that the observed N$_2$O increase in the atmosphere since pre-industrial times is accompanied by a significant isotopic depletion in ^{15}N at both positions in the molecule and in [18]O. Using the data in combination with a firn air diffusion model, the small present rates of change of the isotope

signatures have been precisely quantified, which is important for global isotope budget calculations. Such budget calculations, performed for the present and the pre-industrial atmospheres, reveal that the observed isotopic depletions are not simply due to an increase in the source strength of the isotopically depleted surface sources. In addition, the global average isotopic source signature itself has also decreased since pre-industrial times.

It is interesting to note that ^{15}N has changed similarly at both positions in the molecule due to the strong increase of the global N$_2$O source since pre-industrial times. This is in sharp contrast to the stratospheric N$_2$O sinks where the overall fractionations are much stronger at the central position than at the terminal position. Potentially, these different isotope signatures may be used to discriminate between source and sink (e.g. changes in solar irradiation or stratosphere-troposphere exchange) effects as origin of variations in the N$_2$O mixing ratio on longer time scales, as observed in ice cores. First N$_2$O isotope data on air extracted from ice cores are now becoming available (Sowers, 2001), although they have not yet reached the necessary precision.

Global average isotopic source signatures could not be obtained from direct isotope ratio measurements on N$_2$O sources so far due to the heterogeneity of the sources themselves and the large range of isotope signatures encountered (Gros et al., 2002). The top-down approach presented here provides independent information and should therefore be useful for future research on the global N$_2$O isotope budget. Temporal isotope trends and fractionation constants for stratospheric photolysis and reaction of N$_2$O with O(^{1}D) are well established now. Therefore, future modeling efforts should aim for a more comprehensive and more accurate calculation of the actual back-flux and corresponding isotopic enrichment of stratospheric N$_2$O. Nevertheless, the simple box model approach used here already gives a good representation of the expected global average source signature. The detailed investigation of the stratosphere-troposphere exchange is presently an active field of atmospheric research, and advances in this area in the future will further reduce the uncertainties of top-down budget calculations.

CO_2 data. Bernd Knape helped a lot with the development of the continuous-flow system and the isotope measurements.

References

Battle, M., Bender, M., Sowers, T., Tans, P. P., Butler, J. H., Elkins, J. W., Ellis, J. T., Conway, T., Zhang, N., Lang, P., and Clarke, A. D.: Atmospheric gas concentrations over the past century measured in air from firn at the South Pole, Nature, 383, 231–235, 1996.

Brenninkmeijer, C. A. M., Koeppel, K., Röckmann, T., Scharffe, D. S., Bräunlich, M., and Gros, V.: Absolute measurement of the abundance of atmospheric carbon monoxide, J. Geophys. Res., 106, 10 003–10 010, 2001.

Brenninkmeijer, C. A. M. and Röckmann, T.: Mass spectrometry of the intramolecular nitrogen isotope distribution of environmental nitrous oxide using fragment-ion analysis, Rap. Comm. Mass Spectrom., 13, 2028–2033, 1999.

Cliff, S. S. and Thiemens, M. H.: The $^{18}O/^{16}O$ and $^{17}O/^{16}O$ ratios in atmospheric nitrous oxide: a mass-independent anomaly, Science, 278, 1774–1776, 1997.

Dore, J. E., Popp, B. N., Karl, D. M., and Sansone, F. J.: A large source of atmospheric nitrous oxide from subtropical North Pacific waters, Nature, 396, 33–66, 1998.

Fabre, A., Barnola, J. M., Arnaud, L., and Chappellaz, J.: Determination of gas diffusivity in polar firn: Comparison between experimental measurements and inverse modeling, Geophys. Res. Lett., 27, 557–560, 2000.

Flückiger, J., Dällenbach, A., Blunier, T., Stauffer, B., Stocker, T. F., Raynaud, D., and Barnola, J.-M.: Variations in atmospheric N_2O concentration during abrupt climatic changes, Science, 285, 227–230, 1999.

Griffith, D. W. T., Toon, G. C., Sen, B., Blavier, J.-F., and Toth, R. A.: Vertical profiles of nitrous oxide isotopomer fractionation measured in the stratosphere, Geophys. Res. Lett., 27, 2485–2488, 2000.

Gros, V., Brenninkmeijer, C. A. M., Jöckel, P., Kaiser, J., Lowry, D., Nisbet, E. G., O'Brian, P., Röckmann, T., and Warwick, N.: Use of isotopes, in: Emissions of chemical species and aerosols in the atmosphere, (Ed) Granier, C., in press , Kluwer, Paris, 2002.

Holton, J. R.: On the Global Exchange of Mass between the Stratosphere and Troposphere, J. Atmos Sci., 47, 392–395, 1990.

Houghton, J. T., Ding, Y., Griggs, D. J., Nogueur, M., van der Linden, P. J., Dai, X., Maskell, K., and Johnson, C. A.: Climate Change 2001: The Scientific Basis, Cambridge University Press, 2001.

Johnson, M. S., Billing, G. D., Gruodis, A., and Janssen, M. H. M.: Photolysis of nitrous oxide isotopomers studied by time-dependent hermite propagation, J. Phys. Chem. A, 105, 8672–8680, 2001.

Kaiser, J.: Stable isotope investigations of atmospheric nitrous oxide, Ph.D. thesis, University of Mainz, available at http://archimed.uni-mainz.de/pub/2003/0004/, or Verlag Dr. Hut, Mnchen, ISBN 3-934767-90-7, 2002.

Kaiser, J., Brenninkmeijer, C. A. M., and Röckmann, T.: Intramolecular ^{15}N and ^{18}O fractionation in the reaction of N_2O with O(^1D) and its implications for the stratospheric N_2O isotope signature, J. Geophys. Res., 107, 10.1029/2001JD001506, 2002a.

Kaiser, J., Brenninkmeijer, C. A. M., and Röckmann, T.: Temperature dependence of isotope fractionation in N_2O photolysis, Phys. Chem. Chem. Phys., 4, 10.1039/b204837j, 2002b.

Kaiser, J., Brenninkmeijer, C. A. M., Röckmann, T., and Crutzen, P.: Wavelength dependence of isotope fractionation in N_2O photolysis, Atmos. Chem. Phys., 3, 303–313, 2003.

Kim, K.-R. and Craig, H.: Nitrogen- 15 and oxygen- 18 characteristics of nitrous oxide: A global perspective, Science, 262, 1855–1857, 1993.

Luz, B., Barkan, E., Bender, M. L., Thiemens, M. H., and Boering, K. A.: Triple-isotope composition of atmospheric oxygen as a tracer of biosphere productivity, Nature, 400, 547–550, 1999.

Naqvi, S. W. A., Yoshinari, T., Jayakumar, D. A., Altabet, M. A., Narvekar, P. V., Devol, A. H., Brandes, J. A., and Codispoti, L. A.: Budgetary and biogeochemical implications of N_2O isotope signatures in the Arabian Sea, Nature, 394, 462–464, 1998.

Pérez, T., Trumbore, S. E., Tyler, S. C., Matson, P. A., Ortiz-Monasterio, I., Rahn, T., and Griffith, D. W. T.: Identifying the agricultural imprint on the global N_2O budget using stable isotopes, J. Geophys. Res., 106, 9869–9878, 2001.

Rahn, T. and Wahlen, M.: A reassessment of the global isotopic budget of atmospheric nitrous oxide, Glob. Biogeochem. Cycl., 14, 537–543, 2000.

Rahn, T., Zhang, H., Wahlen, M., and Blake, G. A.: Stable isotope fractionation during ultraviolet photolysis of N_2O, Geophys. Res. Lett., 25, 4489–4492, 1998.

Röckmann, T., Brenninkmeijer, C. A. M., Wollenhaupt, M., Crowley, J. N., and Crutzen, P. J.: Measurement of the isotopic fractionation of $^{15}N^{14}N^{16}O$, $^{14}N^{15}N^{16}O$ and $^{14}N^{14}N^{18}O$ in the UV photolysis of nitrous oxide, Geophys. Res. Lett., 27, 1399–1402, 2000.

Röckmann, T., Kaiser, J., Brenninkmeijer, C. A. M., Crowley, J. N., Borchers, R., Brand, W. A., and Crutzen, P. J.: Isotopic enrichment of nitrous oxide ($^{15}N^{14}NO$, $^{14}N^{15}NO$, $^{14}N^{14}N^{18}O$) in the stratosphere and in the laboratory, J. Geophys. Res., 106, 10 403–10 410, 2001a.

Röckmann, T., Kaiser, J., Crowley, J. N., Brenninkmeijer, C. A. M., and Crutzen, P. J.: The origin of the anomalous or "mass-independent" oxygen isotope fractionation in tropospheric N_2O, Geophys. Res. Lett., 28, 503–506, 2001b.

Röckmann, T., Kaiser, J., Brenninkmeijer, C. A. M., and Brand, W. A.: Gas-chromatography, isotope-ratio mass spectrometry method for high-precision position-dependent ^{15}N and ^{18}O measurements of atmospheric nitrous oxide, Anal. Chem., submitted, 2003.

Rommelaere, V., Arnaud, L., and Barnola, J.-M.: Reconstructing recent atmospheric trace gas concentrations from polar firn and bubbly sea ice data by inverse methods, J. Geophys. Res., 102, 30 069–30 083, 1997.

Schwander, J., Stauffer, B., and Sigg, A.: Air mixing in firn and the age of the air at pore close-off, Ann. Glaciol., 10, 141–145, 1988.

Sowers, T.: N_2O record spanning the penultimate deglaciation from the Vostok ice core, J. Geophys. Res., 106, 31 903–31 914, 2001.

Sowers, T., Rodebaugh, A., Yoshida, N., and Toyoda, S.: Extending records of the isotopic composition of atmospheric N_2O back to 1900 a.d. from air trapped in snow at South Pole, in: 1st international symposium on isotopomers, (Ed) Yoshida, N., Yokohama, Japan, 2001.

Toyoda, S., Yoshida, N., Urabe, T., Aoki, S., Nakazawa, T., Sugawara, S., and Honda, H.: Fractionation of N_2O isotopomers in

the stratosphere, J. Geophys. Res., 106, 7515–7522, 2001.

Trenberth, K. E. and Guillemot, C. J.: The total mass of the atmosphere, J. Geophys. Res., 99, 23 079–23 088, 1994.

Trudinger, C. M., Enting, D. M., Etheridge, D. M., Francey, R. J., Levchenko, V. A., Steele, L. P., Raynaud, D. , and Arnaud, L.: Modeling air movement and bubble trapping in firn, J. Geophys. Res., 102, 6747–6763, 1997.

Turatti, F., Griffith, D. W. T., Wilson, S. R., Esler, M. B., Rahn, T., Zhang, H., and Blake, G. A.: Positionally dependent ^{15}N fractionation factors in the UV photolysis of N$_2$O determined by high resolution FTIR spectroscopy, Geophys. Res. Lett., 27, 2489–2492, 2000.

Warneck, P.: Chemistry of the natural atmosphere, pp. 923, Academic Press, San Diego, 1999.

Yoshida, N. and Toyoda, S.: Constraining the atmospheric N$_2$O budget from intramolecular site preference in N$_2$O isotopomers, Nature, 405, 330–334, 2000.

Yung, Y. L. and Miller, C. E.: Isotopic fractionation of stratospheric nitrous oxide, Science, 278, 1778–1780, 1997.